1- and 2-Photon Fluorescence Anisotropy Decay in Silicon Alkoxide Sol−Gels: Interpretation in Terms of Self-assembled Nanoparticles

Chris D. Geddes,[†] **Jan Karolin, and David J. S. Birch***

The Photophysics Group, Department of Physics and Applied Physics, University of Strathclyde, 107 Rottenrow, Glasgow, G4 ONG, Scotland, UK

Received: August 27, 2001

We have studied the one- and two-photon induced fluorescence anisotropy decay of rhodamine 6G (R6G) during polymerization of tetramethyl orthosilicate (TMOS) approaching the sol-to-gel transition, a time denoted t_g, using time-correlated single-photon counting and femtosecond Ti:sapphire laser excitation. A biexponential decay of fluorescence anisotropy is observed at all times. We propose a different interpretation to the widely accepted view, that fluorescence anisotropy reports solely on molecular viscosity in sol−gels. We think our results are consistent with the presence of both free dye and dye bound to nm-size silica particles rather than just the coexistence of different discrete viscosity domains as reported previously. A corollary of our interpretation is that the microviscosity changes very little from that of the initial bulk sol throughout the sol−gel polymerization. Nanometer-size particles are known from small angle scattering studies to be precursors to gelation in sol−gels over a wide range of conditions and our interpretation might prove to be an important step toward understanding the self-assembly mechanisms of silicon alkoxide based materials at the molecular level. According to our measurements and interpretation, for TMOS at pH 2.3 for example, primary silica particles of ≈0.8-nm mean radius grow by monomer−monomer or monomer−cluster addition to produce larger structures ≈1.1-nm mean radius after one month.
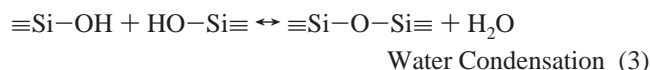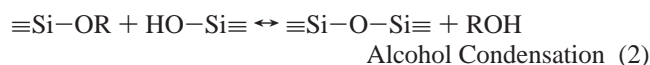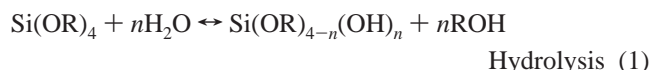
Introduction

The sol−gel process involves the transformation of a liquid-like solution, *the sol*, to *the gel*, a highly porous matrix filled with solvent, through a series of hydrolysis and polycondensation steps. After gel formation, the solvent can be removed and the gel densified to produce solid glass monoliths, which find wide ranging applications in photonics and sensors and, when ground down, as cleaning, polishing, fining, printing, and adhesive agents. The research and industrial importance of sol−gel glasses cannot be overestimated, and yet at the molecular level the structural and dynamical processes involved are still poorly understood.
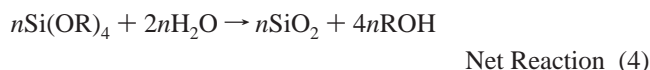
The silica sol−gel process is a room-temperature either organic or inorganic polymerization which is strongly pH and SiO_2 concentration dependent.[1,2] For hydrogels at pH < 2 (acid catalyzed), gelation occurs by means of a series of monomer or intercluster condensation reactions between silanol (−Si−OH) bonds to form ramified siloxane (−Si−O−Si−) clusters. At pH > 8 (base catalyzed), more solid siloxane based particles can grow larger by monomer addition as smaller particles dissolve (Ostwald rippening) or by aggregation. At intermediate pH values of 3−7, both growth mechanisms, under certain conditions, can be observed. Silica gels can typically be produced by two main methods, that is, the hydrolysis and polycondensation of either lithium, sodium, or potassium silicates, either acid or base catalyzed (an *inorganic* polymerization) or from acid or base catalyzed tetrafunctional alkoxides

(an *organic* polymerization). The former gels are frequently referred to as hydrogels and the latter as alcogels in accordance with both the solvents used and condensed. There are many similarities between both processes and similar end products are obtained. The alkoxide alcogel route is the one which has been most used for research into sol−gel processes because it has better defined reactants and is typically simpler to prepare than a hydrogel; the lower cost of the latter makes it more suitable for applications requiring mass production.

In this paper, we concentrate on the alkoxide route, which at the functional group level can be described by three reactions:[2]

$$Si(OR)_4 + nH_2O \leftrightarrow Si(OR)_{4-n}(OH)_n + nROH$$

$$\text{Hydrolysis (1)}$$

$$\equiv Si-OR + HO-Si \equiv \leftrightarrow \equiv Si-O-Si \equiv + ROH$$

$$\text{Alcohol Condensation (2)}$$

$$\equiv Si-OH + HO-Si \equiv \leftrightarrow \equiv Si-O-Si \equiv + H_2O$$

$$\text{Water Condensation (3)}$$

and overall by the net reaction:

$$nSi(OR)_4 + 2nH_2O \rightarrow nSiO_2 + 4nROH$$

$$\text{Net Reaction (4)}$$

where in our case, the alkyl group R is a methyl group. The hydrolysis reaction, eq 1, effectively replaces alkoxide groups with hydroxyl groups, which can then readily condense to produce either water, eq 3, or alcohol, eq 2, where both reactions result in siloxane (Si−O−Si) bonds. Because water and alkoxides are immiscible, a mutual solvent is typically used as a homogenizing agent, for example, an alcohol. As indicated by eqs 1 and 2, alcohol is not just a solvent but can participate in

---

* To whom correspondence should be addressed. E-mail: DJS.Birch@strath.ac.uk. Fax: +44 (0)141 552 2891.
† Present address: Center for Fluorescence Spectroscopy, Department of Biochemistry and Molecular Biology, University of Maryland Biotechnology Institute, 725 West Lombard St., Baltimore, MD 21201.

the reverse esterification and alcoholysis reactions, respectively. The hydrolysis scheme, eq 1, is generally acid or base catalyzed where the rate and nature of polymerization is pH dependent.[2] Other parameters such as temperature, pressure, the type of alcohol used, and the molar H_2O:Si ratio (denoted δ:1) significantly influence the properties of the final gel.[2] It is widely accepted[2] that acid-catalyzed hydrolysis of a tetrafunctional alkoxide with low δ values produces weakly branched *polymeric* type sols whereas base-catalyzed hydrolysis with large δ values produces highly condensed *particulate* sols. Intermediate conditions produce intermediate structures that lie within these boundary conditions.[2]

Fluorescence probe spectroscopy has become an established tool for probing structure and dynamics at the molecular level[3] and has been used extensively for this purpose in the study of sol−gels.[4] In particular, fluorescence depolarization due to Brownian rotation of a molecular probe reports on the local mobility of the probe. Expressed most usually as an anisotropy function, both steady-state and time-resolved, numerous workers have interpreted the changes observed during alkoxide sol−gel polymerization solely in terms of viscosity[5−8] from initial mixing to well beyond the sol-to-gel transition after a time t_g.

Recently, we have reported fluorescence anisotropy decay studies of silica hydrogels during the polymerization of sulfuric acid and sodium silicate solution at pH $\approx$ 1.[9,10] We proposed a model whereby the two anisotropy decay times observed describe the rotation of free dye and dye bound to silica clusters. According to this model, the clusters were found to grow from an initial mean hydrodynamic radius of $\approx$1.5 nm (present within the first twenty minutes of mixing) to a maximum mean radius of $\approx$4.5 nm after $\approx$2000 min, irrespective of t_g. The free dye rotation enabled the microviscosity to be calculated and this was found both before and after t_g to be close to that of the initial bulk sol, that is, $\approx$1−2 cP.

Prior to our work, Narang and co-workers[7] used phase-modulation fluorometry to study R6G in TMOS gels at a sol pH of 4, 6, and 8 and observed two anisotropy decay components from the outset to beyond t_g. These they attributed to the presence of two discrete microdomains of different viscosity. One viscosity of $\approx$2 cP remained more or less constant during polymerization and was associated with free R6G and the other increased during polymerization to a value over an order of magnitude greater than the bulk or microviscosity even prior to t_g. This is perhaps a surprising result as such a large microviscosity disparity might be expected to lead to phase separation, which was not reported. However, there were a number of differences between the work of Narang and ours apart from the sol composition. We had used a different dye, JA120, and worked at pH $\approx$ 1, that is, a positive particle surface charge (the isoelectric point and the point of zero charge for silica lies in the pH range 1−3[1,2]) rather than on the negative charge side (pH > 3).

We have thus revisited the TMOS−R6G system using time-correlated single-photon counting with picosecond resolution and multiphoton excitation to increase the dynamic range over which the decay of fluorescence anisotropy can be observed during sol polymerization. We have also chosen to use a slow gelling sol so that negligible polymerization occurs in the duration of a fluorescence anisotropy decay measurement.

The results we have obtained are presented here and mirror those we observed previously for silica hydrogels[9,10] and suggest that the presence of particles needs to be taken into account when interpreting fluorescence anisotropy data in sol−gels in general. Here, we use the word "particle" loosely to describe

the range of silica clusters, which can occur under different conditions, from ramified to more solid assemblies of silica.

We report here studies for $t < t_g$ and our results are consistent with those reported previously by Narang et al.[7] over this region, but we suggest that the longer and increasing R6G anisotropy decay component corresponds to an increase in hydrodynamic radius because of attachment of the dye to growing silica particles, not an increase in microviscosity, which stays fairly constant.

The case for nanometer-scale silica particles being present and indeed "growing" during sol−gel polymerization is overwhelming from electron microscopy, neutron, X-ray, and light scattering measurements which have been performed in many different laboratories on many different sol compositions.[11−18] Our interpretation of fluorescence anisotropy data reconciles the findings of fluorescence with those of these other techniques and offers a new approach to studying the dynamics and structure of sol−gel glass formation.

Theory

Vertically and horizontally polarized fluorescence decay curves, $F_V(t)$ and $F_H(t)$, orthogonal to pulsed and vertically polarized excitation recorded at different delay times following initial mixing of the sol lead to an anisotropy function $R(t)$[3] describing the rotational correlation function where

$$R(t) = \frac{F_V(t) - F_H(t)}{F_V(t) + 2F_H(t)} \quad (5)$$

If continuous excitation is used, the time dependencies remain unresolved and a weighted average of the time-resolved anisotropies is observed in a multicomponent system such as a sol−gel to give a steady-state anisotropy R.

Our previous analysis of $R(t)$[9,10] for silica hydrogels and that of Narang and co-workers[7] on TMOS showed that the best description was provided by two rotational correlation times τ_{r1} and τ_{r2} in the form

$$R(t) = (1 - f)\, R_0 \exp(-t/\tau_{r1}) + fR_0 \exp(-t/\tau_{r2}) \quad (6)$$

where R_0 is the initial anisotropy. We interpret f as the fraction of fluorescence due to probe molecules bound to silica particles and hence $1 - f$ is the fraction due to free dye in the sol. From the Stokes−Einstein relation, τ_{r1} gives the sol microviscosity $\eta_1 = 3\tau_{r1}kT/4\pi r^3$, where r is the hydrodynamic radius of the dye, and likewise using η_1 and τ_{r2} gives the average silica particle hydrodynamic radius.

By expanding $\exp(-t/\tau_{r2})$ and putting $\tau_{r1} \ll \tau_{r2}$, to reflect the unbound probe molecules rotating much faster than those which are bound to silica particles, then where the fluorescence lifetime $\tau_f \ll \tau_{r2}$ a similar expression to that encountered for the hindered rotation of a fluorophore in a membrane or protein[3] can be expected to hold in a sol−gel, that is, a residual anisotropy is observed

$$R(t) = (1 - f)R_0 \exp(-t/\tau_{r1}) + fR_0 \quad (7)$$

If a fraction of the fluorescence g is attributed to dye bound rigidly within the gel after t_g as well as both free solvated dye and dye bound to silica particles then, if appropriate, eq 6 could be further extended to

$$R(t) = \\ (1 - f - g)R_0 \exp(-t/\tau_{r1}) + fR_0 \exp(-t/\tau_{r2}) + gR_0 \quad (8)$$

Given the potential complexity of the molecular rotations likely to be observed, we chose to also use multiphoton excitation as well as one-photon excitation used previously.[7,9,10] Multiphoton excitation increases the initial value of the fluorescence anisotropy, R_0, and hence the dynamic range over which rotations are observed. This is particularly useful when the fluorescence lifetime is significantly less than the rotational correlation time, as is the case here. For i-photon excitation R_0 can be expressed as[3]

$$R_0 = \frac{2i}{2i + 3}\left[\frac{3}{2}\cos^2\beta i - \frac{1}{2}\right] \tag{9}$$

where β_i is the intramolecular angle between the dominant absorption and emission transition moments. In the collinear ($\beta_i = 0$) case, $R_0 = 0.4$ for $i = 1$ and 0.57 for $i = 2$.

Experimental Section

Materials. Tetramethyl orthosilicate (TMOS), HCl, ethanol, and laser-grade R6G were purchased from the Aldrich Chemical Co. Ltd and were used as received.

Sample Preparation. TMOS based sol−gels were made by mixing tetramethyl orthosilicate, ethanol, water (doubly deionized), and HCl together to produce pH 2.3, 21.91% (w/w) SiO_2 sol−gels (on the basis of complete polymerization of the reactants). The δ value was 2.00, which under stoichiometric conditions would lead to complete hydrolysis and condensation, cf. eq 4. Solutions were initially cooled to <4 °C prior to hydrolysis to minimize any potential solvent boiling because of the exothermic nature of the reaction. A concentrated ethanol stock solution of R6G was used in the preparation to adjust the optical density of the sol to less than 0.1 at λ_{abs}max = 530 nm. 3.5 cm^3 of sol was then cast into a quartz cuvette and sealed throughout to reduce drying, as compared to the sol−gels made by Narang et al,[7] which were opened after 48 h as part of an investigation into the drying process. For all measurements, the sample remained optically transparent such that depolarization due to multiple scattering from particles and pores could be neglected. The gelation time, t_g, was typically 56160−59040 min at ≈20 °C, measured by observing the time for 15 mL of sol to start peeling away from the sides of a sealed 50-mL glass sample bottle (Fisher Scientific UK) to the time when the sol had set firm.

Fluorescence Measurements. Steady-state fluorescence anisotropy measurements were performed on a FluoroMax-2, ISA instruments New Jersey, equipped with dichroic sheet polarizers (Halbo Optics). The excitation and emission wavelengths were 480 and 530 nm, respectively. Absorption measurements were performed on a Perkin-Elmer UV/VIS spectrophotometer, Lambda 2.

Two and white light one-photon femtosecond excitations were achieved using a Coherent RegA 9000/Mira 900 regeneratively amplified Ti:Sapphire laser (repetition rate 250 kHz; excitation pulse duration ≈120 fs; center wavelength 800 nm; energy per pulse ≤4 μJ). The fluorescence anisotropy decay curves were collected using the well-known time-correlated single-photon-timing technique.[19] The instrument and measurement of multiphoton excited fluorescence anisotropy decays have been described previously,[20] recent additions being a faster photon timing detector (Hamamatsu cooled MCP−PMT model R3809U-50) and discriminator (EG&G Ortec model 9327). The overall instrumental response was ≈100 ps fwhm. Two-photon-excited R6G fluorescence was the wavelength selected by using a 800-nm cutoff filter, which excluded the laser fundamental. The laser

power dependence of the fluorescence confirmed the two-photon nature of the excitation.[20]

For the time-resolved one-photon-excited fluorescence experiments, white light was generated in a Ti:sapphire crystal. The excitation wavelength from the white light continuum was selected by a 500 ± 10 nm interference filter (Comar Instruments, UK), and the fluorescence emission was observed through a 550-nm long-pass filter. For all experiments, the temperature was regulated at 20 ± 1 °C. The typical measurement time taken to record the anisotropy decay was ≈30 min, sufficient to accumulate a maximum count per channel of 10,000−20,000 in the difference function $F_V(t) - F_H(t)$ (cf. eq 5).

Impulse reconvolution analysis of fluorescence anisotropy decays was performed using the IBH reconvolution software library with the normalized χ^2 value, weighted residuals, and autocorrelation function used as a measure of goodness of fit.[19] Magic angle polarization, 54.7°, was selected for all R6G fluorescence lifetime measurements.

Bulk Viscosity Measurements. Bulk viscosities, η_b, were determined for sols just up to t_g and also for solvents in probe volume determinations, using two Ostwald Viscometers (Fisher Scientific) in the range 0−6 and 6−30 cP. The viscometers were initially calibrated with a standard of known viscosity and density at various temperatures, that is, water. For the viscosity measurements of sols, the temperature was maintained at 20 °C. The density of a 21.91% SiO_2 (w/w), pH 2.3, $\delta = 2.00$ sol at 1160 min, 20 °C, was 0.923 g cm^{-3} (mean of five measurements).

The Fluorescent Probe. R6G has a fluorescence quantum yield of ≈0.95 in alcohol and a high two-photon absorption cross section at 800 nm of ≈10^{-48} cm^4 s.[21] R6G is well known to be an isotropic rotor, and the fluorescence anisotropy decay in a range of known viscosity solvents enabled the probe's volume (and subsequently radius) to be checked. A value of 5.3 ± 0.3 Å was found for both one- and two-photon excitation. This value is consistent with previous measurements[22−24] and also corresponds well to a molecular radius of 5.6 Å obtained from the theoretical rotational times of an oblate rotator with semi-axes of 7 and 2 Å.[24,25] Hence, for ease of comparison, we also used in our calculations the value of 5.6 Å used by Narang et al.[7]

Results

We studied the TMOS sol at a low pH (≈2.3) which gave a long gel time (t_g ≈ 56160−59040 min) to observe changes in the time-resolved fluorescence anisotropy using both one- and two-photon excitation with the maximum degree of statistical precision. A SiO_2 (w/w) concentration of ≈22% sol was used ($\delta = 2$). Narang et al[7] studied ≈14% SiO_2 (w/w) sols ($\delta \approx 11$) at pH 4, 6, and 8 with t_g ≈ 240−290, 50−60, and <15 min, respectively, as remeasured by the authors.

Figure 1 shows the bulk viscosity η_b (A) and steady-state anisotropy R (B) from our measurements as a function of polymerization time, pt. These results follow expected trends and when considered in the context of the different time scale of gelation, the steady-state anisotropy is consistent with that reported at earlier times by Narang et al.[7] Our sample remained sealed throughout, preserving optical quality over the long gelation period and minimizing solvent loss during syneresis. This is reflected in the gradual change in steady-state anisotropy which we observe, as compared to the more rapid changes in the sols prepared by Narang et al, which were opened after 48 h.[7] We observed the fluorescence spectrum of R6G in the sol
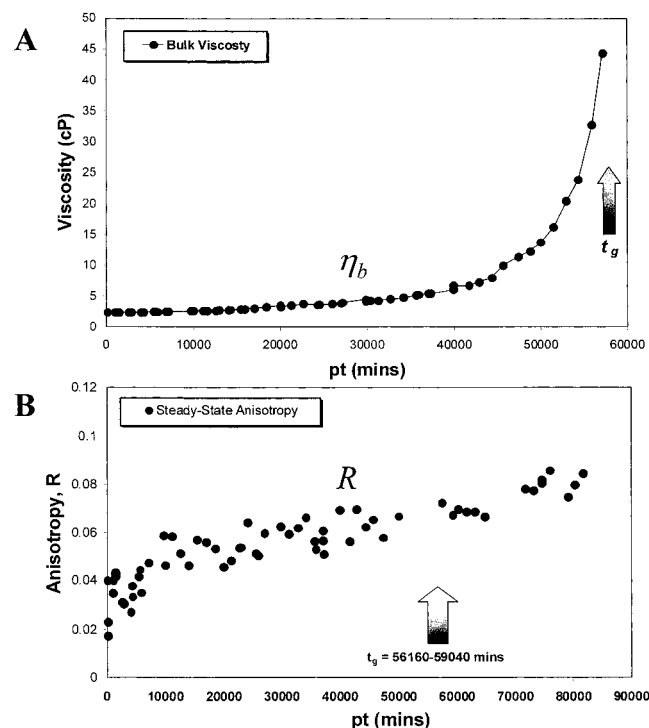
A

B

Figure 1. (A) Bulk viscosity η_b and (B) steady-state anisotropy, R, as a function of polymerization time, pt, for the TMOS sol at pH $\approx$ 2.3, t_g = 56160$-$59040 min and SiO$_2$ (w/w) concentration $\approx$ 22%.

TABLE 1: R6G Anisotropy Decay Analysis Using Two Rotational Times (Eq 6) for $a \approx$ 22 % SiO$_2$, pH 2.3 TMOS Sol$-$Gel, as a Function of pt^a

	fitting to eq 6			
pt (mins)	τ_{r1}/s	τ_{r2}/s	R_o	χ^2
3986	3.47e^{-10}	9.71e^{-10}	0.501	1.12
15941	3.40e^{-10}	1.42e^{-9}	0.488	1.21
18611	3.45e^{-10}	1.01e^{-9}	0.512	1.23
20176	2.80e^{-10}	1.14e^{-9}	0.506	1.14
23156	3.19e^{-10}	1.48e^{-9}	0.490	1.44
24546	2.98e^{-10}	1.39e^{-9}	0.546	1.20
25656	3.19e^{-10}	1.67e^{-9}	0.534	1.26
27376	3.64e^{-10}	1.73e^{-9}	0.530	1.15
28626	2.89e^{-10}	1.46e^{-9}	0.481	1.20
30231	2.96e^{-10}	1.59e^{-9}	0.540	1.27
31836	3.30e^{-10}	1.54e^{-9}	0.514	0.97
33156	3.81e^{-10}	1.86e^{-9}	0.540	1.19
34566	2.93e^{-10}	1.77e^{-9}	0.502	1.32
35766	3.19e^{-10}	2.18e^{-9}	0.498	1.15
36131	2.58e^{-10}	1.57e^{-9}	0.495	1.12
37371	2.98e^{-10}	1.92e^{-9}	0.501	1.35
38751	3.13e^{-10}	2.09e^{-9}	0.453	1.42
40266	3.18e^{-10}	1.91e^{-9}	0.489	1.17
44706	2.97e^{-10}	1.85e^{-9}	0.488	1.24

^{a} pt is polymerization time (min). λ_{ex} = 800 nm.

to red shift during the polymerization, for example, at 70 min $\lambda_{max} \approx$ 537 nm and at 40,000 mins $\lambda_{max} \approx$ 544 nm as compared to a $\approx$6-nm blue shift observed after $\approx$29,000 mins by Narang et al.[7] This is presumably related to the different drying rates.

The fluorescence decay of R6G in the sol was found to be well described by 3.70 $\pm$ 0.05 ns throughout, which compares well with the value of 3.85 $\pm$ 0.2 ns reported by Narang et al.[7] While the steady-state emission spectrum shifts slightly during sol polymerization, the absorption spectrum and excited-state fluorescence decay kinetics were seen to be unaffected.

Table 1 gives the results of analyzing the anisotropy decay curves using two rotational correlation times (cf. eq 6). Figure 2 shows a typical impulse reconvolution fit of eq 6 to $F_V(t)$ $-$
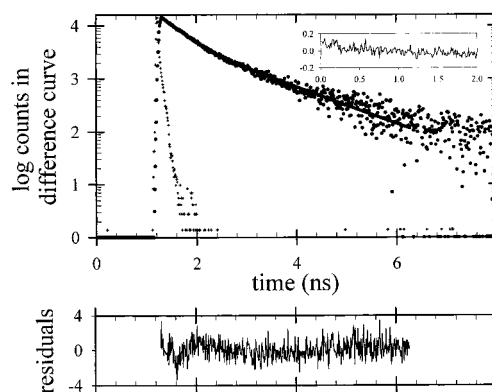

Figure 2. Impulse reconvolution fit of two rotational times to the difference $F_V(t)$ $-$ $F_H(t)$ for the R6G doped TMOS sol after a polymerization time of 40266 min using two-photon excitation at 800 nm. The instrumental response function ($<$100 ps fwhm), autocorrelation function (insert), and weighted residuals are also shown. The channel width is 8.7 ps.
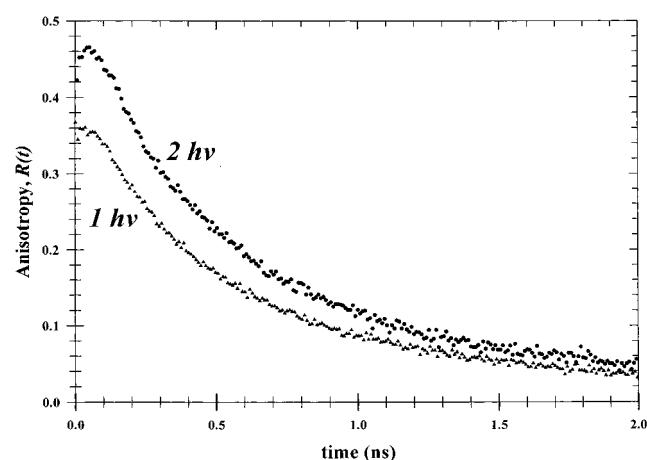

Figure 3. Anisotropy decay for the R6G doped TMOS sol after a polymerization time of 40266 min using two-photon excitation at 800 nm and one-photon femtosecond excitation at $\approx$500 nm.

$F_H(t)$ for one data set during the polymerization. A comparison of the χ^2 value for the alternative model of one rotational correlation time and a residual anisotropy (eq 7) showed the two correlation time model to be more appropriate; the same conclusion being reached in the phase-modulation work of Narang et al.[7] Fitting to eq 8 (includes an additional "g" term for dye fixed in a gel) gave no significant improvement in the χ^2 value. The two-photon excited R_0 value obtained of $\sim$0.5 demonstrates a useful increase beyond the one-photon maximum value of 0.4 (cf. eq 9 and Figure 3). As polymerization proceeds, the little changing value of the faster rotational correlation time, τ_{r1}, (from Table 1 $\approx$ 300 ps) and its near constant fractional contribution to the total fluorescence (from Figure 4 $\approx$70$-$80%) agree closely with the findings of Narang et al.[7]

The inescapable conclusion when comparing our results with those obtained by Narang et al.[7] is that despite the different measurement techniques and sols, there is excellent agreement. Only in the long decay component τ_{r2} might there be a notable difference. (One actual numerical value and a series of graphical points for τ_{r2}, which look to approach 10 ns before drying, were given in reference 7. Our maximum value of τ_{r2} is $\sim$2 ns, cf. Table 1). To check the possibility that in using two-photon excitation we have in some way influenced the rotational correlation time (e.g., by heating), we performed control experiments at lower power using one-photon femtosecond pulses from a white light continuum at 500 nm. The results for
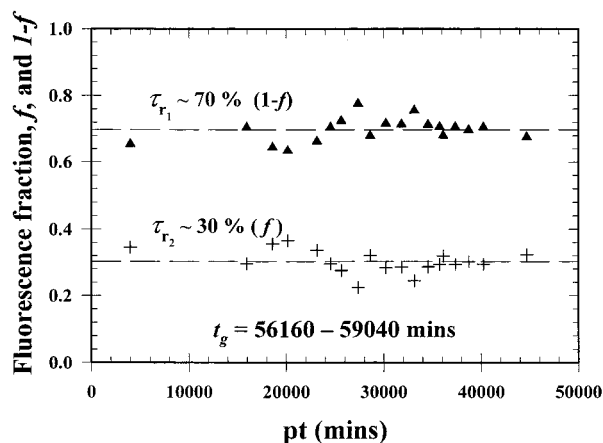
Figure 4. Fraction of the total fluorescence $1 - f$ associated with the fast rotational correlation time τ_{r1}, ▲, and f associated with the slow rotational time τ_{r2}, +, for the R6G doped TMOS sol during polymerization.

TABLE 2: A Comparison of the Rotational Correlation Time τ_{r2}, Eq 6, Using Femtosecond 1- and 2-Photon Excitation for the TMOS Sol as a Function of Polymerization Time, pt[a]

pt	τ_{r2}/ns 1 $h\nu$	τ_{r2}/ns 2 $h\nu$
1263	0.61 ± 0.19	0.82 ± 0.36
2775	0.87 ± 0.41	0.66 ± 0.17
11400	1.28 ± 0.77	1.20 ± 0.66
24360	1.84 ± 0.85	1.71 ± 0.63
41663	2.30 ± 1.16	1.79 ± 0.77

[a] The pt values for 1- and 2-photon measurements are the mean values of both times, where measurements were typically of <30 min duration and taken sequentially. Errors shown are three standard deviations.

τ_{r2} obtained for both one- and two-photon excitation (of an identical but separate TMOS sol to that for which data are presented in Table 1) are shown in Table 2. The results show no evidence of a systematic discrepancy and are consistent given that pt is slightly different for the one- and two-photon measurements, which were taken sequentially. This is consistent with the findings of multiphoton excited fluorescence anisotropy studies in various media in several laboratories.[26] Hence, we attribute any difference in τ_{r2} between the work of Narang et al and our results to differences in the sols used (see next section).

This presentation of results has centered only on anisotropy decay curve parametrization and so far has made no comment on interpretation of the meaning of τ_{r1} and τ_{r2}, which are discussed in the next section.

Discussion

Since the rotational time of R6G in simple alcohols and water is reported to be in the range $\approx$100−400 ps,[22−24] we ascribe τ_{r1} in the TMOS sol to free dye rotating in the liquid phase in agreement with the conclusion reached previously.[7] Figure 5 compares the bulk viscosity η_b, the microviscosity η_1 of our TMOS sol from τ_{r1}, and a second microviscosity η_2 calculated from τ_{r2}, assuming the free dye is rotating in a second viscous environment, that is, the fluorescence anisotropy decays are interpreted solely in terms of viscosity changes.[7] This has been the widely held belief, but here we offer another and perhaps potentially more useful interpretation. Figure 6 uses η_1 determined from τ_{r1} in the Stokes−Einstein equation to determine a silica particle radius, not a second microviscosity, from τ_{r2}. According to this interpretation of fluorescence anisotropy, the
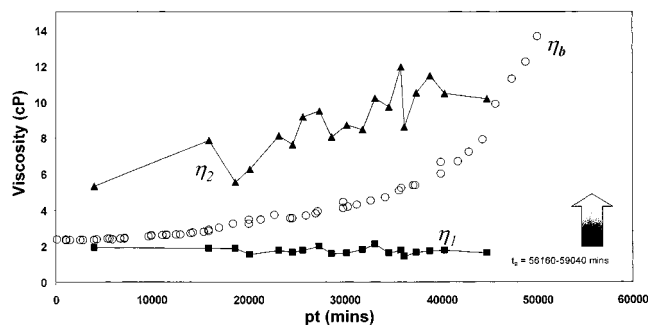

Figure 5. Bulk viscosity η_b and microviscosities η_1 and η_2 determined from rotational correlation times τ_{r1} and τ_{r2}, respectively (cf. eq 6), assuming they both relate to R6G rotating in two different fluid environments in the TMOS sol.
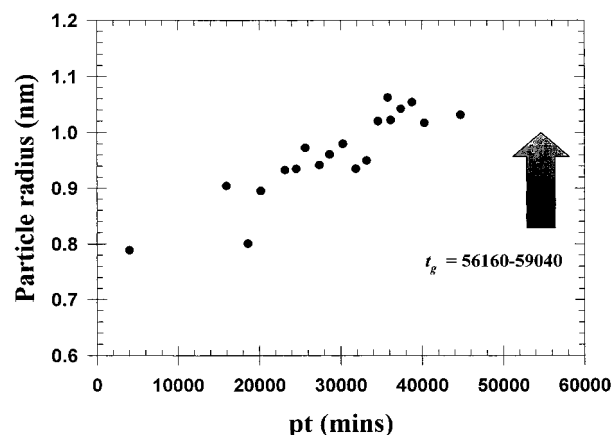

Figure 6. Silica particle radius, ●, (nm) as a function of polymerization time, pt, for the TMOS sol determined from τ_{r2} and the microviscosity given by τ_{r1} (cf. eq 6). The error in the particle radius is $\approx$ ± 0.1 nm.

particle radius in our TMOS sol increases from $\approx$0.8 nm to 1.1 nm after one month of polymerization, that is, before t_g, which is broad in the range 56160−59040 min. Although small, Figure 6 shows this 0.3-nm growth to be measurable.

We find the particle interpretation more plausible for several reasons. First, Figure 5 shows that for our sol, η_2 would need to be up to an order of magnitude greater that η_1. The viscosity ratio looks to require to be made even greater to account for the slow dye rotation in the measurements presented by Narang and co-workers.[7] The existence of two viscosity domains from the outset in a sol seems to us an implausible explanation, and there are no reports of a phase separation prior to t_g. A reanalysis of Figure 6 of reference 7 using our particle interpretation predicts an initial particle radius, r, of $\approx$0.8 nm growing to $\approx$1.5 nm after 100 mins, consistent with our measurements. We associate the fact that $r \sim 1.5$ nm ($\equiv \tau_r \sim 10$ ns) from reference 7 is greater than $r \sim 1.1$ nm ($\equiv \tau_r \sim 2$ ns) which we observe, with the pH of 6 in reference 7 leading to larger particles than would be expected at the pH of 2.3 which we have used.[2] Moreover, a fit of the equivalent growth function derived from reference 7 to $r \sim 1 - e^{-kt}$ gives $k \sim 8 \times 10^{-4}$ s^{-1}, that is, a similar value to what we reported for an acidic hydrogel of 15% (w/w) SiO$_2$.[9,10] Second, the existence of nm particles, which grow at different rates (including not growing) depending on conditions, is indisputable from scattering studies of many types of sols including alkoxides.[11−18] Third, although it could be argued that the presence of particles is only circumstantial evidence, the evidence for many types of dyes in general binding to SiO$_2$ and xanthene dyes such as R6G, in particular, is well established.[4] Given that sol−gel silica matrixes trap R6G well, it would seem surprising if this affinity was not present with

the silica particles in a sol. Moreover, R6G is a cationic dye; the isoelectric point of silica is at pH $\approx$ 1–3, and as pH increases above the isoelectric point, the SiO_2 particles become increasingly negatively charged. Recently, time-resolved fluorescence anisotropy data was interpreted for stable colloidal silica particles of negative charge (Du Pont's colloidal LUDOX range) in terms of 7-nm diameter SiO_2 particles with a totally bound quinolinium dye concentration[27] and 18-nm particles using a mixture of free and bound rhodamine B.[28]

When we interpreted the fluorescence anisotropy decay in acidic silica hydrogels in terms of particle growth from 1.5 to 4.5 nm,[9,10] the dye concerned (JA120) was only gradually taken up by the silica particles such that f was time-dependent. In TMOS–R6G, the constant f suggests that a constant partition of dye between the particle and solvent is established very rapidly (cf. Figure 4). There are several specific differences between these two systems, which might explain the kinetic difference. For example, in our TMOS work an ethanolic R6G solution was used in the preparation to homogenize the H_3O^+, whereas the hydrogels reported previously were post-doped several minutes after preparation, and this may explain the time dependence of f. Conversely, methanol is produced (eq 2) in the TMOS polymerization but not with hydrogels, and the greater solubility of R6G in methanol may lead to a redissolution of the dye offsetting its take up by silica particles. Any differences in dye fluorescence quantum yield may also contribute. It is not possible to fully remove all the R6G from the final gel by repeated washing with ethanol. Moreover, the value of ~300 ps we obtain for τ_{r1} (cf. Table 1) is close to what might be expected for the rotational correlation time of free R6G in the water/alcohol sol we have here.

The upshot is that f most probably relates to a particle bound or free dye partition in TMOS, but we cannot totally rule out the possibility that all the dye is taken up by the particles early on, and τ_{r1} describes bound dye wobbling on the particle. In this case η_1 would refer to a vicinal microviscosity and f would reflect the relative fluorescence quantum yields of R6G associated with the two rotational times corresponding to the dye fixed and wobbling on the particle. Although the vicinal viscosity close to a silica particle could be different to the microviscosity sensed by the free dye, the $r \sim \eta^{-3}$ dependence reduces the effect on the measured particle radius. Even if it is argued that dye trapped in the interior and dye wobbling on the surface of a silica particle could be thought of as two viscosity domains, the particle size still comes into play in the anisotropy decay via Brownian rotation. Although the dimensions of the dye (radius 0.56 nm) might make a significant contribution to the overall particle radius, intercalation would reduce the dye obtrusion.

Of course we are encountering a distribution of particle sizes here, and there may well be more than one microviscosity present (if vicinal is included as well as bulk). Nevertheless, our main point that particles need to be considered when interpreting fluorescence anisotropy in sols still holds. This is particularly true before t_g, though at or soon after t_g the majority of the volume of a sol–gel is still in the fluid phase, that is, gelation is the minimum amount of material used to span the containing vessel and form a solid network, rather than the maximum.

Conclusions

We have demonstrated that the parametrization of fluorescence anisotropy decay in sols in terms of two rotational correlation times can be explained equally well by considering the presence of silica particles. The evidence points to such an explanation of changes in the anisotropy decay during sol–gel polymerization being more likely than the widely accepted view of the coexistence of differing viscosity domains. We are not suggesting that the decay of fluorescence anisotropy reflects the presence of particles in *all* kinds of sols under *all* conditions and for *all* dyes, and we are not suggesting that there can never be more than one microviscosity present.

Nevertheless, the particle interpretation of fluorescence anisotropy decay reconciles various pieces of evidence in a manner which might contribute in a new way to moving on our understanding of the dynamics and structures involved in sol-to-gel transitions at the molecular level. Understanding the steps whereby particle size and growth translates into pores depends on being able to perform nanometer metrology on the sol and gel. The interpretation we propose offers the opportunity to be able to monitor sol–gels in situ with sub-nanometer resolution. Moreover, because dye immobilized in a gel does not depolarize fluorescence (cf. eq 8), it is possible to study particle size well after t_g, a major potential advantage over scattering techniques where gel scattering can distort the scattering function. Similarly, fluorescence anisotropy can be performed at high silica densities whereas other fluorescence particle techniques for studying nanoparticles, such as fluorescence correlation spectroscopy and fluorescence recovery after photobleaching, require dilute sols, which can cause de-polymerization.

References and Notes

(1) Iler, R. K. *The Chemistry of Silica*; John Wiley and Sons: New York, 1979.

(2) Brinker, C. J.; Scherer, G. *Sol–Gel Science, The Physics and Chemistry of Sol–Gel Processing*; Academic Press: San Diego, 1989.

(3) Lakowicz, J. R. *Principles of fluorescence spectroscopy*, 2nd ed.; Plenum: New York, 1999.

(4) Dunn, B.; Zink, J. I. *J. Chem. Mater.* **1997**, *9*, 2280.

(5) Winter, R.; Hua, D. W.; Song, X.; Mantulin, W.; Jonas, J. *J. Phys. Chem.* **1990**, *94,* 2706.

(6) Dunn, B.; Zink, J. I. *J. Mater. Chem.* **1991**, *6*, 903.

(7) Narang, U.; Wang, R.; Prasad, P. N.; Bright, F. V. *J. Phys. Chem.* **1994**, *98*, 17.

(8) Qian, G. D.; Wang, M. Q. *J. Phys. D: Appl. Phys.* **1999**, *32,* 2462.

(9) Geddes, C. D.; Birch, D. J. S. *J. Non-Cryst. Solids* **2000**, *270*, 191.

(10) Birch, D. J. S.; Geddes, C. D. *Phys. Rev. E* **2000**, *62*, 2977.

(11) Himmel, B.; Gerber, T.; Burger, H. *J. Non-Cryst. Solids* **1987**, *91*, 122.

(12) Orcel, G.; Hench, L. L.; Artaki, I.; Jonas, J.; Zerda, T. W. *J. Non-Cryst. Solids* **1988**, *105*, 223.

(13) Boonstra, A. H.; Meeuwsen, T. P. M.; Baken, J. M. E.; Aben, G. V. A. *J. Non-Cryst. Solids* **1989**, *109*, 153.

(14) Winter, R.; Hua, D. W.; Thiyagarajan, P.; Jonas, J. *J. Non-Cryst. Solids* **1989**, *108*, 137.

(15) Byers, C. H.; Harris, M. T.; Williams, D. F. *Ind. Eng. Chem. Res.* **1987**, *26*, 1916.

(16) Matsoukas, T.; Gulari, E. *J. Colloid Interface Sci.* **1988**, *124*, 252.

(17) Gerber, T.; Himmel, B.; Hübert, C. *J. Non-Cryst. Solids* **1994**, *175*, 160.

(18) Himmel, B.; Burger, H.; Gerber, T.; Olbertz, A. *J. Non-Cryst. Solids* **1995**, *185*, 56.

(19) Birch, D. J. S.; Imhof, R. E. In *Topics in fluorescence spectroscopy*; Lakowicz, J., Ed.; Plenum: New York, 1991; Vol. 1.

(20) Volkmer, A.; Hatrick, D. A..; Birch, D. J. S. *Meas. Sci. Technol.* **1997**, *8*, 1339.

(21) Fischer, A.; Cremer, C.; Stelzer, E. H. K. *Appl. Opt.* **1995**, *34*, 1989.

(22) Eichler, H.; Klein, U.; Langhans, D. *Chem. Phys. Lett.* **1979**, *67*, 21.

1- and 2-Photon Fluorescence Anisotropy Decay

J. Phys. Chem. B, Vol. 106, No. 15, 2002 **3841**

(23) Wijnaendts Van Resandt, R.; Maeyer, L. *Chem. Phys. Lett.* **1981**, *78*, 219.

(24) Porter, G.; Sadkowski, P.; Tredwell, C. *Chem. Phys. Lett.* **1977**, *49*, 416.

(25) Fleming, G.; Morris, J.; Robinson, G. *Chem. Phys.* **1976**, *17*, 91.

(26) Birch, D. J. S. *Spectrochim. Acta, Part A* **2001**, *57*, 2313.

(27) Geddes, C. D.; Apperson, K.; Birch, D. J. S. *Dyes Pigm.* **2000**, *44*, 69.

(28) Smith, T. A.; Irwanto, M.; Haines, D. J.; Ghiggino, K. P.; Millar, D. P. *Colloid Polym. Sci.* **1998**, *276*, 1032.